



**Research Paper / Makale**

**Methodology for Determination of Small Intestine Phantom Length  
Based on Computerized Tomography Images**

Mustafa YAZ<sup>a</sup>, Seda Benli KAYNAK<sup>b</sup>

<sup>a</sup>Electrical and Electronics Engineering Department, Yozgat Bozok University, Yozgat, TURKEY

<sup>b</sup>Electrical and Electronics Engineering Department, Selçuk University, Konya, TURKEY

[mustafa.yaz@bozok.edu.tr](mailto:mustafa.yaz@bozok.edu.tr)

Received/Geliş: 01.04.2021

Accepted/Kabul: 20.06.2021

**Abstract:** Congenital or acquired lesions leading to a large loss of intestinal mass leads to the formation of short bowel syndrome. The occurrence of bowel incompetence is also mostly due to short bowel syndrome. Intestinal length knowledge is needed in bowel diseases that are shortened by various causes such as bowel insufficiency. o date, there are few studies on the calculation of small bowel length in the literature based on computed tomography (CT) images. In this paper, a methodology is proposed to calculate the length of small intestinal phantoms by using CT images. First, pre-processing is carried out by applying morphological processes to the CT image. Center points of the CT image, converted into binary using thresholding methods, are determined by using the region growing method. By writing the equation created in the second-order of the center points, the correct ordering of the center points is obtained by finding the errors in each cycle and ordering the minimum ones. Thus, by calculating and summing the distances between the center points, the length of the small intestinal phantom is found. Three small intestinal phantoms are utilized for validating the proposed methodology.

**Keywords:** Small intestinal segmentation, Short bowel syndrome, Image processing, Computed tomography

**Bilgisayarlı Tomografi Görüntülerine Dayalı İnce Bağırsak Fantom  
Uzunluğunu Belirleme Metodolojisi**

**Öz:** Büyük bir bağırsak kütlesi kaybına yol açan doğuştan veya edinilmiş lezyonlar, kısa bağırsak sendromunun oluşumuna yol açar. Bağırsak yetmezliğinin ortaya çıkması da çoğunlukla kısa bağırsak sendromuna bağlıdır. Bağırsak yetmezliği gibi çeşitli nedenlerle kısalan bağırsak hastalıklarında bağırsak uzunluğu bilgisine ihtiyaç vardır. o tarih, literatürde bilgisayarlı tomografi (BT) görüntülerine dayanan ince bağırsak uzunluğunun hesaplanmasıyla ilgili az sayıda çalışma vardır. Bu yazıda, BT görüntülerini kullanarak ince bağırsak fantomlarının uzunluğunu hesaplamak için bir metodoloji önerilmiştir. İlk olarak, CT görüntüsüne morfolojik işlemler uygulanarak ön işleme gerçekleştirilir. Eşikleme yöntemleriyle ikiliye dönüştürülen CT görüntüsünün merkez noktaları bölge büyütme yöntemi kullanılarak belirlenir. Merkez noktalarının ikinci sırasına göre oluşturulan denklem yazılarak, her döngüdeki hataları bularak ve minimum olanları sıralayarak merkez noktalarının doğru sıralaması elde edilir. Böylece merkez noktalar arasındaki mesafeler hesaplanıp toplanarak ince bağırsak fantomunun uzunluğu bulunur. Önerilen metodolojiyi doğrulamak için üç ince bağırsak fantomu kullanılır.

**Anahtar Kelimeler:** İnce bağırsak bölütleme, Kısa bağırsak sendromu, Eşikleme, Bilgisayarlı tomografi

**1. Introduction**

Today, engineering applications find solutions to most of the problems encountered in the field of health with the developing technology methods [1].

How to cite this article

Yaz M., Kaynak Benli S., "Methodology for Determination of Small Intestine Phantom Length Based on Computerized Tomography Images" El-Cezeri Journal of Science and Engineering, 2021, 8 (3); 1202-1214.

Bu makaleye atıf yapmak için

Yaz M., Kaynak Benli S., "Bilgisayarlı Tomografi Görüntülerine Dayalı İnce Bağırsak Fantom Uzunluğunu Belirleme Metodolojisi" El-Cezeri Fen ve Mühendislik Dergisi 2021, 8 (3); 1202-1214.

ORCID ID: <sup>a</sup>0000-0001-7042-7649; <sup>b</sup>0000-0002-6377-5941

With the development of technology, it is observed that the applications of medical imaging, disease modelling and biomedical engineering also increase [2]. In the diagnosis of many diseases, imaging techniques that are frequently used in the biomedical field and analysis of the images obtained are used. Biomedical engineering is preferred in the treatment and diagnosis of small bowel diseases [3]. Loss of more than 50-75% of the normal small bowel length results in a significant reduction of the functional absorbent area in the intestine [4,5]. It causes a basis for the formation of various metabolic and physiological disorders (weight loss, loss of water, and vitamin deficiencies) [6,7]. Intestinal length information is an important factor for patients with intestinal diseases such as intestinal insufficiency and short bowel syndrome [8,9]. Although the intestinal length and diameter are important in the medical management of patients with bowel insufficiency (therapeutic) and operation management [10], it is difficult to accurately measure the physical size of the small intestine except for the surgical event [11,12]. However, even the predictions of the small bowel length during the operation are not reliable because the measurement depends on many factors, including the surgical procedure and stretching during measurement in the intestine [13]. In the experimental environment, the size and anatomy of the mouse used in the mouse model with short bowel syndrome limit the measurements of the small bowel length and pre-mortem [14,15]. These restrictions severely limit the ability of clinical interventions and experimental treatments to understand the effects on gut length without using a noninvasive method of assessing small bowel length [4]. Computer-aided systems are needed because these processes take a lot of time.

To find the small bowel length, it is necessary to segment the small intestine. There are no methods reported in the literature for using three-dimensional computerized tomography (CT) images in the segment of the small intestine. Direct segmentation of CT scans of the small intestine is difficult for four main reasons. Firstly, it is very close to other abdominal organs such as muscle, blood vessels, kidneys, and liver in small intestinal computerized tomography scans. Secondly, their density distributions and tissues are similar to other abdominal organs [4]. Thirdly, the small intestine has a very complex structure. Finally, the small intestine may be in different positions in two CT scans of the same patient due to its moving structure. These four features make it difficult to distinguish the small intestine from other organs, or even to predict a very complex model [4,16].

This study is aimed to find the length of the small intestine phantom based on CT images. Four small intestine phantoms were prepared from four hoses of different sizes and shapes. Three-dimensional (3D) images were obtained by taking computerized tomography of these phantoms. Then they were stored in DICOM format [17] and were loaded into the MATLAB software. An algorithm has been developed to calculate the approximate length of the small intestine phantoms using various image processing techniques. The shortest intestine phantom was taken into consideration for the development of methodology. Then this methodology was tested by using the other three phantom images.

This paper is organized in the following way: Section 2 presents the proposed methodology for the calculation of small intestine phantom length by using CT images. Section 3 provides the results obtained by using four small intestine phantoms. Finally, Section 4 presents the conclusions.

## 2. Material And Methods

In this study, computerized tomography (CT) images of phantoms were taken into binary format. The reason for converting the imported CT image into a binary image is that the binary image can be processed very quickly. In this conversion, the global thresholding method, one of the image thresholding methods, is used. The global thresholding method is used because we want to select a threshold value based on the image's intensity values, not the edge information that is the physical properties of the image. The noise in the image was cleaned and applied to the image by using

various morphological processes. The size of the structural elements used during the morphological processes was tried in the dimension algorithm which gave the best results by trying.

Utilizing the following steps, the locations of the center points were determined and their lengths were found.

- The threshold value to be used for the separation of the points into groups is tried and the best value is used.
- The region growing method is used for image segmentation. This method is used because the region magnification is an image segmentation method where neighboring pixels are added to the corresponding region according to similarity criteria. The initial seed pixel is determined and the region magnification method is applied.
- A second-order equation is designed to make the correct order of center points and the closest choice was made. The equation passing through 5 center points is tried before the equation is created. Then, the equation passing through 10 points is used in the algorithm and it is determined that the equation created with 10 points is more successful. At the end of the application, the moving points are applied to increase the success of the center points.

Figure 1 shows the flowchart of the method used to obtain binary images. Firstly, CT images are converted into dual images by using thresholding methods. Morphological processes are applied to the double image and filled. Erosion and expansion processes are applied with three-dimensional structural elements. Parts other than image are destroyed by labeling.

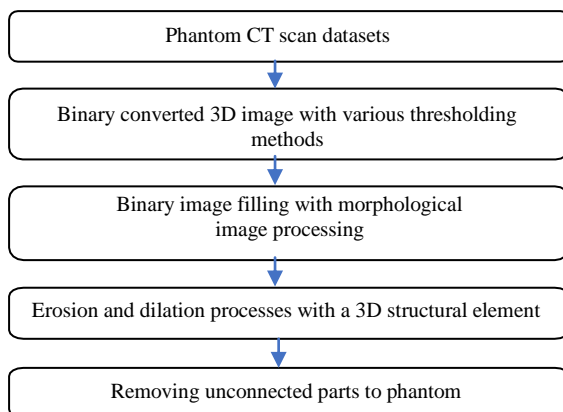


**Figure 1.** Obtaining a binary 3D image of the phantom



**Figure 2.** The small intestine phantom (Phantom 1) was used for the development of the methodology.

In the following subsections, we explain the methodology by using the CT image of gray-colored hose, as shown in figure 2, performed in the Radiology Department of Gülhane Medical Faculty, Faculty of Health Sciences, University of Health Sciences, Turkey. The actual length of the hose is 73.1 cm. CT images of this phantom were acquired in DICOM data format.

### 2.1 Applying the Threshold Method

The image must be converted into a binary image for easy operation. First, the global thresholding method is used. In this way, the program part which has the appropriate threshold value for converting the data into the black and white image is formed as a function. As a result, the threshold value was found to be 176. With this value, the image in the uint16 data type was converted into a black and white image. Figure 3 shows an image of 20 sections selected from 182 sections.

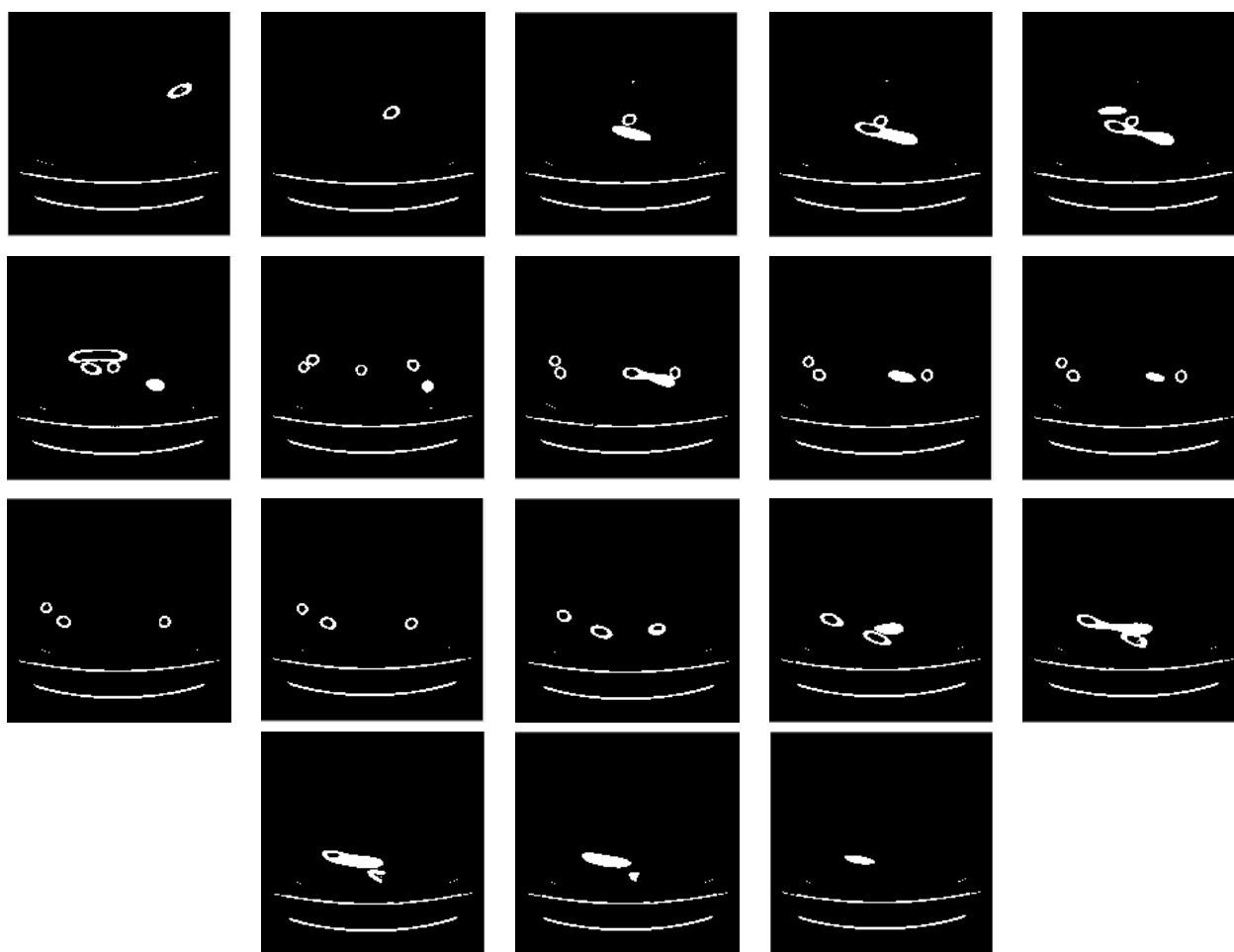


**Figure 3.** Section of Phantom 1 translated into the binary image.

In these images, the inside of the hose is black. In binary terms, it corresponds to the value zero.

### 2.2 Applying Some Morphological Operations To The Obtained Binary Image

In the binary coded CT image, the inside of the hose is filled with white to convert the black parts to white. To separate the parts that touch each other in the sections, all sections were eroded by selecting the structural element disc. In the erosion of the image, the labeling process was performed. In the images, the area was calculated to eliminate the noise that may occur outside the hose. The area information was calculated from the morphological features in the tagged image. By

selecting the address of the maximum area, the noisy part was removed. The structural element was selected in the form of disk size 2, and all sections were subjected to dilatation by the “imdilate” command. The size of the three-dimensional image 512x512x182 was simplified because it causes a long time to run applications. Dimensions were reduced by half to 256x256x91. All subsequent algorithms were applied to this variable. The minimized image was eroded by a 4-radius structural element in the form of a disc. Sections originated from the erosion process are shown in Figure 4

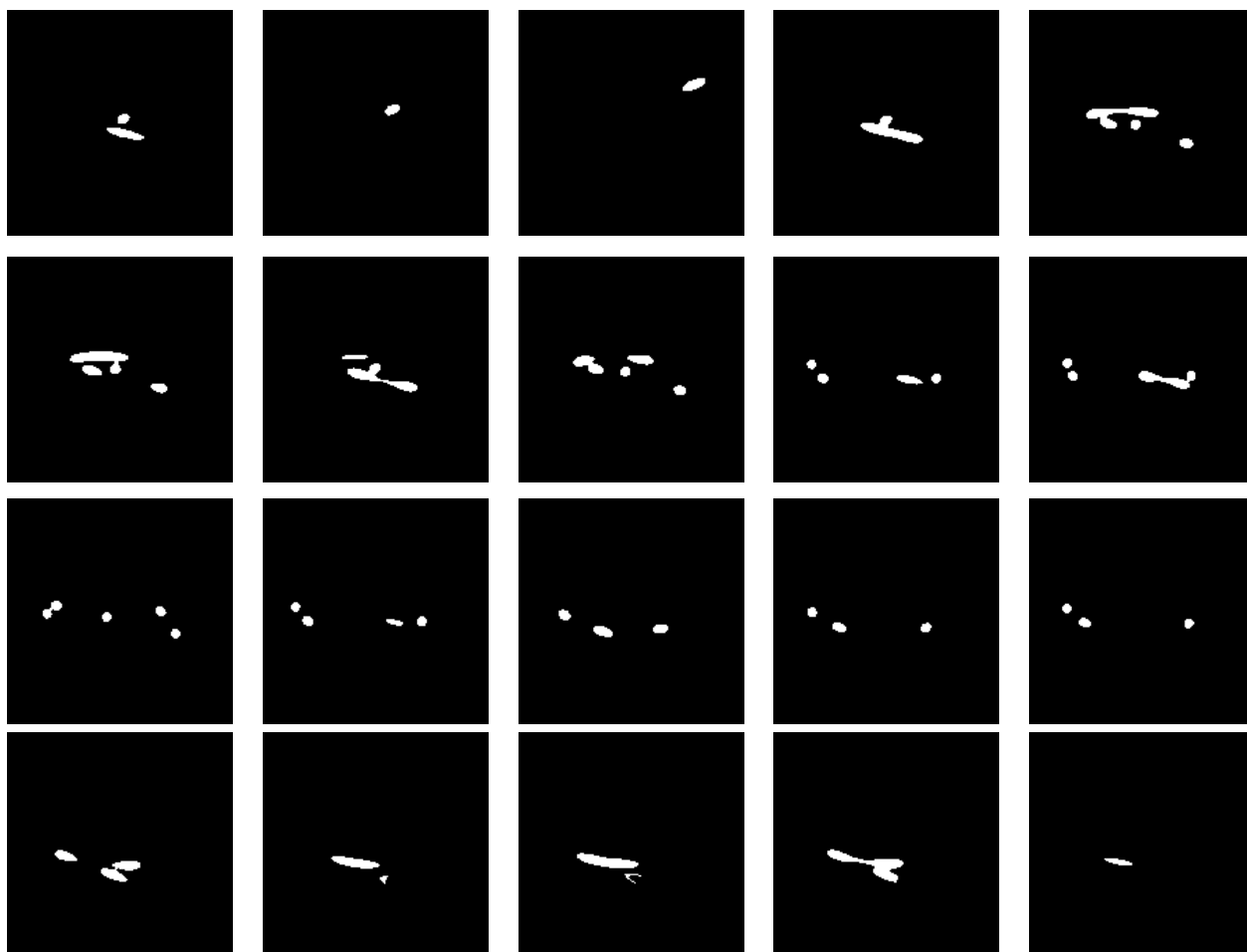


**Figure 4.** Sections originated from the erosion process

### 2.3 Determining Center Points

The purpose of determining the center points in the phantom CT image is to find the phantom length. Once the center points have been determined, the aim will be achieved by finding the distance between the points with all the points.

The size information of the image resulting from the erosion shown in Figure 4 was recorded in a variable. The sum of all pixel values was found. The zero matrices was created with dimensions of image 256x256x91. It was assigned as a three-dimensional matrix structural element of an 8x8x8 where all pixels are 1. The point with the coordinates (8, 208, 11) was selected as the seed point in the image and this point was assigned the value of 1. Starting from this point, the 8x8x8 dimension element was used for expansion and dilation.

The continuously enlarged matrix has intersections with the previous matrix in the loop. The difference between the image and the intersecting region was taken and the component is labeled

with the “bwlabel” command. The center point was determined Centroid center point from the morphological features. The magnification was continued until the entire image was equal to the area of the image. 182 center points were found as shown in Figure 5.

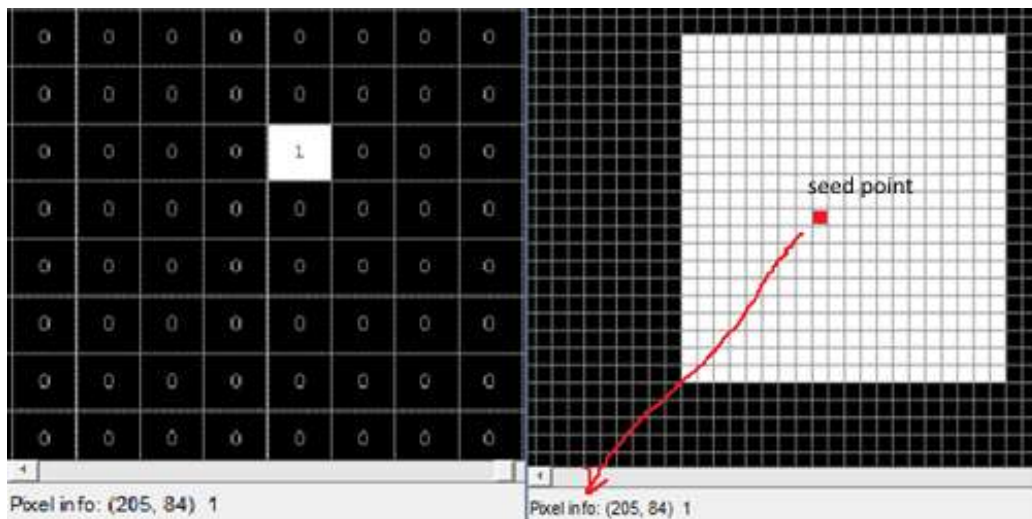


**Figure 5.** Selected seed point and the enlarged region around the seed point

### 2.4 Calculation of Euclidean Distances of Center Points

Row, column, and section information of center points; the row information is recorded in column 1, column information is in column 2, section information is in column 3. In column 4, the index number from 1 to 182 is given. The row, column, section information of the first center point found by the region magnification method is assigned to the first line. Euclidean distances between point 1 and the other 181 points are calculated and the minimum distance from them is assigned to the second row. In this way, all center points are sequenced. Table 1 shows located center points.

**Table 1.** Located center points

Row	Column	Section	Index Number
206	89	11	1
203	90	11	2
199	92	9	3
...	...	...	...
103	145	80	182

Line 1 means that the first center point is the pixel in the 11th section in the three-dimensional image, the 206th line in the 89th column. The most recent center point of the morphological processes is assigned to the first row.

**Table 2.** Sequenced center points according to Euclidean distance-based on the last point.

Row	Column	Section	Index Number
103	145	80	1
114	150	80	2
114	157	76	3
...	...	...	...
206	89	11	182

By calculating the Euclidean distances between these points and the remaining points, the point with the minimum distance is assigned to the second row. In this way, all other points are also arranged. The last row is taken as the first and the sequence is reversed. Table 2 depicts sequenced center points according to Euclidean distance-based on the last point.

### 2.5 Segmentation by Threshold Value

Indexes of the points that are arranged according to the Euclidean distance and the points of the Euclidean distance below 4 mm are assigned to different columns in the same row. In the case of a value greater than 4 mm, a different group is passed to a row and this index is saved.

Thus, the indices of the center points were divided into groups and each group is recorded in the form of 49-element cell arrays in rows. Based on the last order of the specified center points in the same order as the Euclidean distance of 4 mm threshold smaller than the same row in the same row were placed in different columns, 4 mm larger than the different line by moving each group was placed on different lines. Thus, the indices of the center points were divided into groups from the beginning to the end and each group was recorded in 51-element cell arrays in rows. Sequences sorted separately based on the first and the last center points were combined into a single variable.

To be able to make an array from this composite structure, a new variable was created and the first line was joined to assign the indices in the line with the most elements. By taking the difference between this line and other lines, the line with the largest difference was assigned to the second row. The loop continues until all of the indices of the center points are aligned. The result was recorded in the structure of 48-element cell arrays. In this variable, the information of the first and last indices in all rows was saved into two variables, in the size of 48x2. Figure 6 shows the segmentation by threshold value after determining center points.

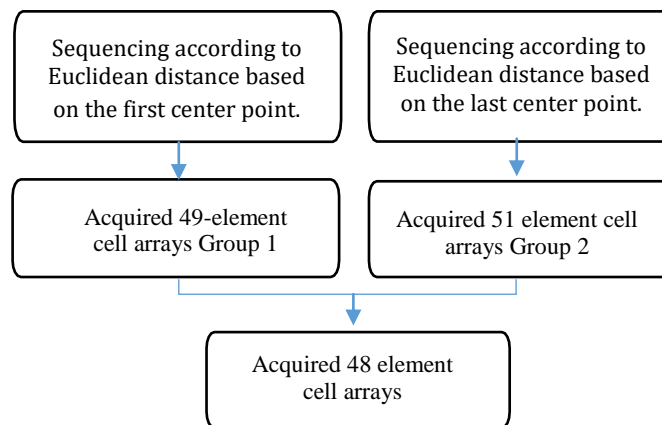


**Figure 6.** Segmentation by threshold value after determining center points

### 2.6 Creating a Second Order Equation

After calculating the Euclidean distance of the center points, it is necessary to create a quadratic equation to be sorted with high accuracy. In the matrix where the first and the last points are registered, 10 of the central points with the indices in the first row and two of the second-degree equations are created.

Equation 1 with coefficients,  $a_0, a_1, a_2, a_3, a_4, a_5, a_6, a_7, a_8$ , is created.

$$Z_n = a_0x^2 + a_1x^2y + a_2x^2y^2 + a_3x + a_4xy + a_5xy^2 + a_6y + a_7y^2 + a_8 \quad (1)$$

$$n = 0..9$$

Since the equation is formed from 10 center points, a 10x9 matrix is obtained by writing row and column information of 10 indices into x and y unknowns in the Zn equation as shown in Equation 2.

$$[x^2 + x^2y + x^2y^2 + x + xy + xy^2 + y + y^2 + 1]_{10 \times 9} * \begin{bmatrix} a_0 \\ a_1 \\ a_2 \\ a_3 \\ a_4 \\ a_5 \\ a_6 \\ a_7 \\ a_8 \end{bmatrix}_{9 \times 1} = \begin{bmatrix} z_0 \\ z_1 \\ z_2 \\ z_3 \\ z_4 \\ z_5 \\ z_6 \\ z_7 \\ z_8 \\ z_9 \end{bmatrix}_{10 \times 1} \quad (2)$$

The values of 10 points are obtained by writing in the matrix created in the size of 10x9. The coefficients are also assigned to a 9x1 matrix. The product of coefficients and unknowns  $z = z_0 + z_1 + z_2 + z_3 + z_4 + z_5 + z_6 + z_7 + z_8 + z_9$  is the index information of the indices which are inserted as a 10x1 size matrix. To obtain the coefficients from this equation, with the least-squares method;

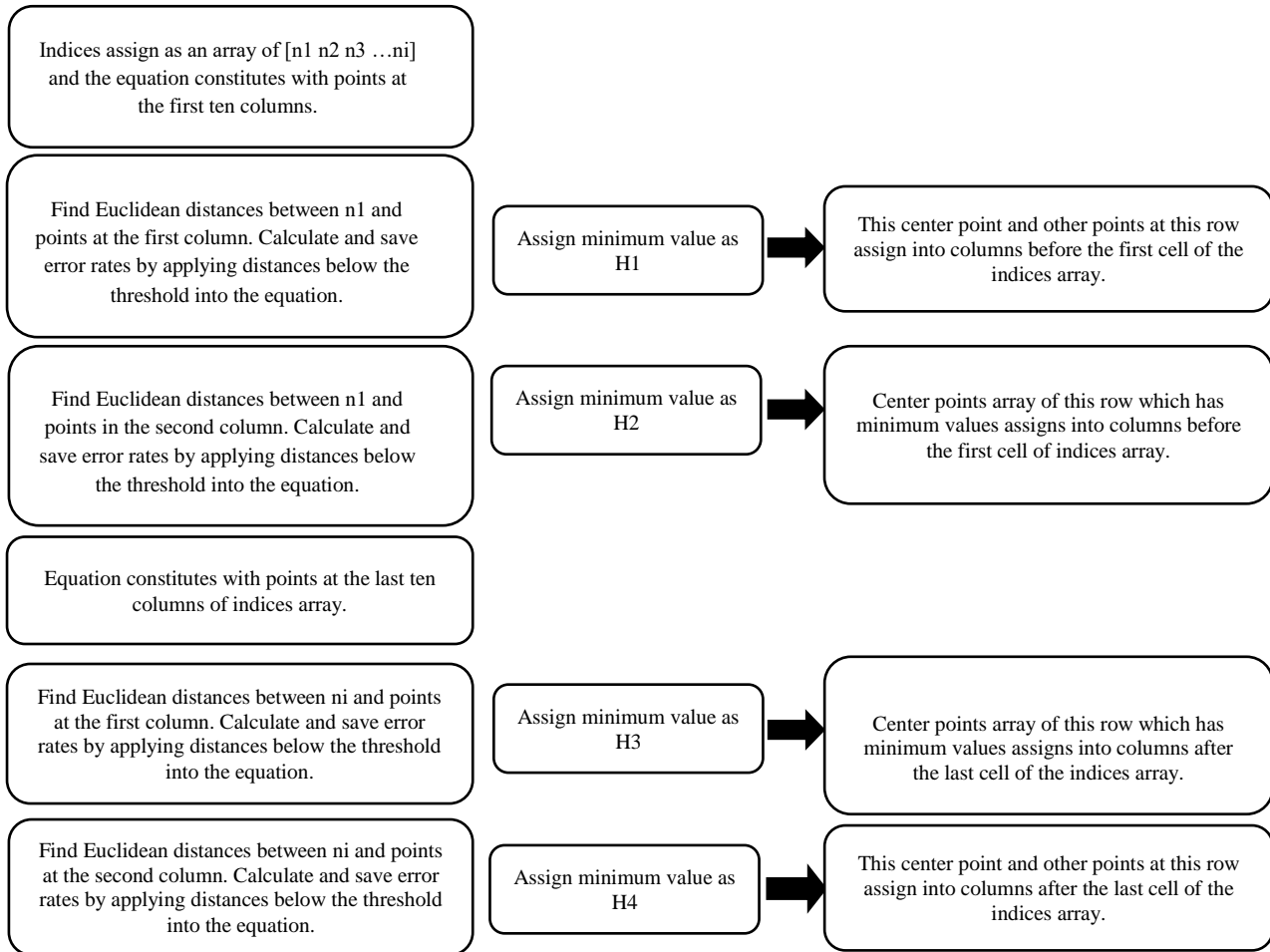
The equation  $Coefficient = ((X^T * X) * X^T)^{-1} * z$  is used. Here,  $a_0, a_1, a_2, a_3, a_4, a_5, a_6, a_7, a_8$  are calculated.

Figure 7 shows the steps of sequence processing by equation. Initially, the first line in the first column contains the Euclidean distances with the other center points in this column and is saved. All points in the line where the point is smaller than the threshold value (7 mm) are written to the generated equation and the z value is found. The difference between the actual value and the value z is calculated. By taking the frames of these differences, the average errors are recorded in a variable and there is a minimum value. H1 is registered with the variable name.

Secondly, the first row is recorded by calculating the Euclidean distances between the center point in the first column and all the center points in the second column. The ones that are smaller than the threshold value are written to the equation and there is an average square error. The minimum H2 is saved with the variable name. The second-order equation is created by 10 points taken from the center and is found by using this second-order equation. The first line is recorded by calculating the Euclidean distances between the center point in the second column and all the center points in column 1. The mean value of the threshold is written to the equation and the mean square error is found. The minimum value is saved as H3.

Again, the first line is recorded with the center point in the second column and the Euclidean distances between the remaining points in the second column. The ones with the threshold value are written in the equation from the beginning to the mean and the mean square error is found. The minimum value among H1, H2, H3, and H4 is saved as min\_error. As the minimum H1 is the distance between the first point of the array and one of the points in the 1st column, the indices in this group are reversed and added before the first cell of the array. As the minimum H2 is calculated by the distance between the first point of the array and one of the points in the 2nd column in other words the last element of the other array, the indices in this group are added before the first cell of the array directly. As the minimum H3 is the distance between the first point of the 2nd column and one of the points in the 1st column, the indices in this group are added after the last cell of the array directly.





**Figure 7.** Steps of sequence processing by equation acquired 48 element cell arrays

As the minimum H4 is the distance between the first point of the 2nd column and one of the points in the 2nd column, the indices in this group are reversed and added after the last cell of the array directly. Figure 8 depicts acquired 48 element cell arrays after segmentation.

$n_1$	$n_2$	$n_3$	$\dots$	$n_i$
$\dots$	$\dots$	$\dots$	$\dots$	$\dots$
$n_a$	$n_b$	$n_c$	$\dots$	$n_j$

**Figure 8.** Acquired 48 element cell arrays after segmentation



**Figure 9.** Three hoses (yellow, blue, and green, respectively) were used as small intestine phantoms (Phantom 4, Phantom 3, Phantom 2, respectively) for validating the proposed methodology.

The center points in the first and last column of this cell line are shown as two columns in a variable. If no group is smaller than the threshold value, i.e., if the min\_error variable is empty, the Euclidean distances registered as M1, M2, M3, M4 are checked and the minimum value is selected. When one of H1, H2, H3, H4 is selected, dots are aligned in the same logic frame. The coordinated coordinates are assigned to the variable xx.

The distance between each of the center points arranged as the last operation is calculated and collected to find the length of the phantom.

### 3. Results and Discussion

Figure 9 shows three hoses that are considered small intestine phantoms. In this section these small intestine phantoms are used for validating the proposed methodology explained in detail in the previous section.

To determine the length of the small intestine phantom, Phantom 2 (green phantom) is studied first. Data files from the DICOM format were obtained from the phantom images taken from CT images. These files were then converted into binary to be used in the MATLAB program. The CT image of Phantom 2 has 182 sections. There are 512 lines and 512 columns in each section of this three-dimensional image. The image is uint16 data type and its voxel thickness is 2 mm. The phantom length is determined by following the following steps: 1. converting the image into the binary format by using the thresholding method, 2. finding the central points by using morphological operations, 3. arranging the distance according to the shortest distance by taking the Euclidean distance of the center points, 4. segmenting this sequence with the threshold value, 5. re-comparing to the Euclidean distance by the threshold value criteria and 6. placing the minimum defective ones by placing them in the second-order equation. If any two points are expressed as x and y, and the voxel thicknesses are indicated by VS, the Euclidean distance between all the points found is calculated by formula 3.

$$\text{Euc\_distance} = \sqrt{(VS_1 * (x_{1,1} - y_{1,1}))^2 + (VS_2 * (x_{1,2} - y_{1,2}))^2 + (VS_3 * (x_{1,3} - y_{1,3}))^2} \quad (3)$$

By summing these distances, the total phantom length is found in millimeters. The total length in cm is expressed in Equation 4.

$$\text{Total Length} = \frac{\text{sum (Euc\_distance)}}{10} \quad (4)$$

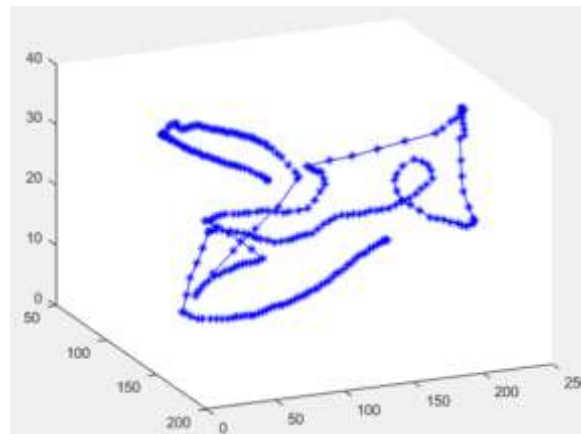


**Figure 10.** Three-dimensional representation of the center points of Phantom 1.

All of the operations performed in this section were also applied to the CT images of different shapes of hoses shown in Figure 9 together with their actual lengths. The result obtained after the first application of the method to Phantom 1 is shown in Figure 10.

The length of Phantom 1 shown in Figure 11 is calculated as 75.03 cm, while the actual length is 73.1 cm. The length of Phantom 2 (green phantom), whose real length is 128 cm, is calculated as 134.6 cm. Figure 11 shows the result obtained by the algorithm.

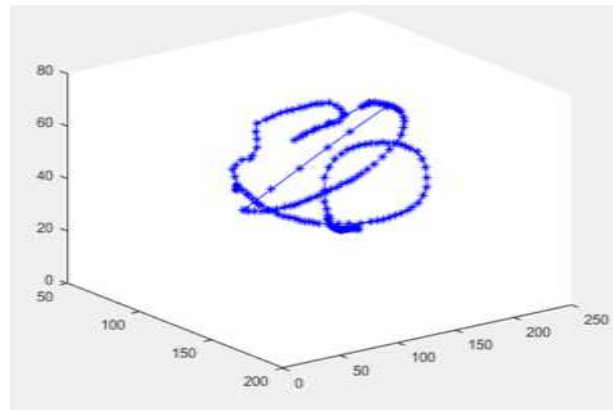


**Figure 11.** Three-dimensional representation of the center points of Phantom 2 (green phantom).

The actual length of Phantom 3 (yellow phantom) is 298 cm and its length is calculated as 281.7 cm. Figure 12 shows the center points of Phantom 4 (yellow phantom) as a result of the algorithm.

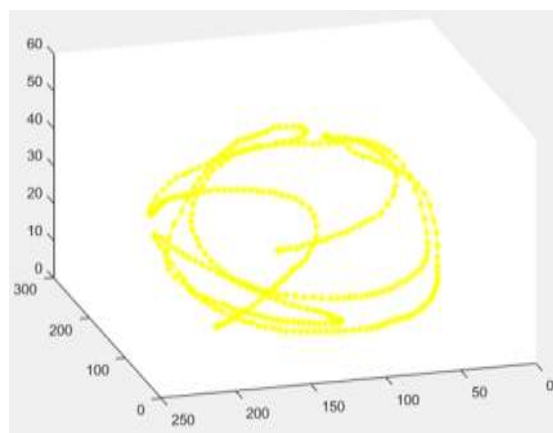


**Figure 12.** Three-dimensional representation of the center points of Phantom 3 (yellow phantom).

The length of Phantom 4 (blue phantom), which has the actual length of 180 cm, is found to be 177.50 cm as a result of the algorithm. Figure 13 shows the center points of the blue phantom as a result of the algorithm.

While the actual length of Phantom 1 (gray) was 73.13 cm, it was calculated as 75.03 cm. According to this result, the phantom length can be determined with an accuracy of approximately 97.46 %. The lengths of the other phantoms, whose actual lengths are 128 cm, 180 cm, and 298 cm, respectively, were measured by the algorithm used in the study and were calculated as 134.6 cm, 174.0 cm, and 281.7 cm, respectively. These results and success rates are provided in Table 3.

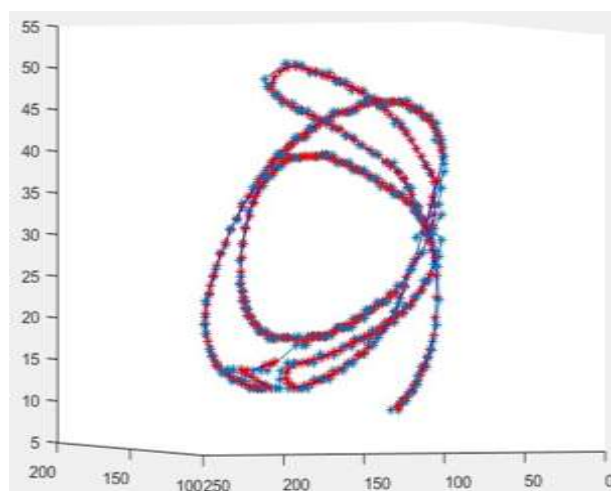


**Figure 13.** Three-dimensional representation of the center points of Phantom 4 (blue phantom).

Table 3 shows the performance rates for four phantom lengths. When Table 3 is examined, the best achievement is seen in Phantom 1, the shortest phantom. The reason for Phantom 4's high error rate is that it is much longer than the others. Phantom 4 has a much-curved structure, which caused the error rate to increase.

**Table 3.** Performance rates for phantom lengths.

		Actual Length	Calculated Length	Error (cm)	Error (%)	Accuracy (%)
Phantom(gray)	1	73.13	75.03	+1.90	2.54	97.46
Phantom(green)	2	128.00	134.60	+6.60	4.91	95.09
Phantom (blue)	3	180.00	174.00	-6.00	3.34	96.66
Phantom (yellow)	4	298.00	281.70	-16.30	5.47	94.53

#### 4. Conclusion

Intestinal length knowledge is very important in bowel diseases that are shortened by various causes such as bowel insufficiency. To date, no study has been reported on the calculation of the length of the small intestine in the literature-based computerized tomography (CT) images. This paper provides a methodology for determining the length of the small intestine phantoms by using CT images. The methodology proposed in this paper has aimed to help doctors in finding the intestinal length without too much intervention in the human body. Results provided in this paper provide an important step towards finding the intestinal length from small intestine phantoms by using CT images. On the other hand, further studies are still necessary to be carried out on the real small intestine in light of the results provided in this paper.

#### Author(s) Contribution

The authors confirm contribution to the paper as follows: study conception and design: M.Y. and S.B.K.; data collection: M.Y. and S.B.K.; analysis and interpretation of results: M.Y.; draft manuscript preparation: S.B.K. All authors reviewed the results and approved the final version of the manuscript.

#### Conflict of Interest

The authors in this publication confirm that they have NO affiliation or affiliation with any organization or organization with any financial interest (such as remuneration; educational grants;

participation in speaker offices; membership, employment, consultations, stock ownership). or other equity interest; and expert testimony or patent-licensing arrangements) or non-financial interest (such as personal or professional relationships, affiliations, knowledge or beliefs) in the topics or materials discussed in this paper.

## References

- [1]. Bozkurt, Y., Özkan, H. G., Karayel, E. Eklemeli İmalat Teknolojilerinin Tıbbi Ekipmanların Üretiminde Kullanımı. *El-Cezeri*, 8(2), 962-980.
- [2]. Sivari, E., Civelek, Z. Genel Anesteziye Kullanılan Propofolün Başlangıç Dozunun Bulanık Mantık ile Tahmini. *El-Cezeri Journal of Science and Engineering*, 2019,6(3), 808-816.
- [3]. Öziç, M. Ü., Özşen, S. 3B Alzheimer MR Görüntülerinin Hacimsel Kayıp Bölgelerindeki Voksel Değerleri Kullanılarak Sınıflandırılması. *El-Cezeri Journal of Science and Engineering*, 2020, 7(3), 1152-1166.
- [4]. Wilson, N.A., et al., A Novel Approach to Calculating Small Intestine Length Based on Magnetic Resonance Enterography, 2017,225(2): 266-273.
- [5]. Grandi, F., et al., Composite Scaffolds Based on Intestinal Extracellular Matrices and Oxidized Polyvinyl Alcohol: A Preliminary Study for a New Regenerative Approach in Short Bowel Syndrome., *Biomed Research International*.
- [6]. Levin, D.E., et al., A Living Bioreactor, for the Production of Tissue-Engineered Small Intestine.,*Springer.*, 2013, 299-309.
- [7]. Grikscheit, T.C., et al., Tissue-Engineered Small Intestine Improves Recovery After Massive Small Bowel Resection, 2004, 240(5): 748.
- [8]. Spencer, A.U., et al., Pediatric Short Bowel Syndrome: Redefining Predictors Of Success, *National Library of Medicine, PubMed.gov*, 2005 242(3): 403.
- [9]. Sala, F.G., et al., A Multicellular Approach Forms A Significant Amount Of Tissue-Engineered Small Intestine In The Mouse. 2011, 17(13-14): 1841-1850.
- [10]. Cromeens, B.P., et al., Production Of Tissue-Engineered Intestine From Expanded Enteroids, 2016, 204(1): 164-175.
- [11]. O'Keefe, S.J., Nutritional Issues In The Short Bowel Syndrome-Total Parenteral Nutrition, Enteral Nutrition And The Role Of Transplantation”, *The Importance of Nutrition as an Integral Part of Disease Management. Karger Publishers.* 2015, 75-90.
- [12]. Donohoe, C.L. and J.V.J.t.s. Reynolds, Short Bowel Syndrome. 2010, 8(5): 270-279.
- [13]. Sulkowski, J.P. and P.C.J.P. Minneci, Management Of Short Bowel Syndrome, 2014, 21(1): 111- 118.
- [14]. Helmroth, M.A., et al., Intestinal Adaptation Following Massive Small Bowel Resection In The Mouse, *National Library of Medicine, PubMed.gov*, 1996, Nov;183(5):441-9.
- [15]. Tacchino, R.M.J.S.f.O. and R. Diseases, Bowel Length: Measurement, Predictors, And Impact On Bariatric And Metabolic Surgery, *Elsevier*, 2015, 11(2): 328-334
- [16]. Yang, X., X. Ye, and G.J.I.T.O.B.E. Slabaugh, Multilabel Region Classification And Semantic Linking For Colon Segmentation In Ct Colonography, *IEEE Transaction of Biomedical Engineering*, 2015, 62(3): 948-959
- [17]. D.A. Clunie, *DICOM Structured Reporting*, PixelMed Publishing, Pennsylvania, 2000